

2023

Investigating the KshB V246S Mutation in the KshAB Protein Complex Found in Mycobacterium Tuberculosis

Malika Cruickshank
Bridgewater State University

Follow this and additional works at: https://vc.bridgew.edu/undergrad_rev

Recommended Citation

Cruickshank, Malika (2023). Investigating the KshB V246S Mutation in the KshAB Protein Complex Found in Mycobacterium Tuberculosis. *Undergraduate Review*, 17, p. 9-22.
Available at: https://vc.bridgew.edu/undergrad_rev/vol17/iss1/5

This item is available as part of Virtual Commons, the open-access institutional repository of Bridgewater State University, Bridgewater, Massachusetts.
Copyright © 2023 Malika Cruickshank

Investigating the KshB V246S Mutation in the KshAB Protein Complex Found in *Mycobacterium Tuberculosis*

MALIKA CRUICKSHANK

Abstract

This research centered on studying the interactions between the KshA and KshB subunits of the 3-ketosteroid-9 α hydroxylase (KshAB) protein complex found in *Mycobacterium tuberculosis* (*M. tuberculosis*). Interactions between the two protein subunits were computationally explored using the protein docking program ClusPro and a location in the KshB subunit at Val 246 was found to be in proximity with nearby amino acids in the KshA subunit. This was determined to be a possible location for docking the protein complex. Val 246 of KshB was mutated into a serine residue to explore changes in the electron transfer pathway upon disruption of this interaction. The V246S KshB protein was successfully overexpressed in *E. coli* cells and purified by Ni-NTA chromatography. Initial enzyme kinetic analysis of the mutated protein complex is now underway. Future research will allow a deeper investigation into whether this mutation will inhibit the flow of electrons from the KshB subunit to the KshA subunit. The long-term goal is to design small molecules that can inhibit the electron flow in the native protein complex that would serve as antibiotics against *M. tuberculosis* infection. unit. The long-term goal is to design small molecules that can inhibit the electron flow in the

native protein complex that would serve as antibiotics against *M. tuberculosis* infection.

Introduction

According to the Centers for Disease Control¹ in 2020, *Mycobacterium tuberculosis*, more commonly known as the bacterium that causes the disease tuberculosis or TB, was the leading infectious disease killer in the world despite being preventable and treatable, killing approximately 1.6 billion people per year. TB is a lung disease commonly believed to be spread from kissing, shaking hands, or any other form of contact with another person, but that's not the case, an infected individual would have to cough, sing, or speak to an uninfected person for it to spread². There are also two forms of tuberculosis called tuberculosis disease, or the active form, and the latent infection. An individual with a latent infection typically isn't even aware that they have the bacteria in them since it doesn't cause any noticeable impacts on their day-to-day life. Patients with tuberculosis disease, however, have been found in higher concentrations in developing countries with weaker healthcare systems since it's harder to access the drugs to control the disease. While the disease is treatable using specific antibiotic drug regimens, if not taken properly, the

bacteria can become resistant to the drugs and evolve into MDR (multi-drug resistant) or XDR (extensively drug-resistant) cases^{3,4}. Most people believe that tuberculosis is no longer a prominent disease since the coverage of it is typically eclipsed by the annual flu virus as well as more recently the COVID-19 pandemic⁵, but it still has very high case numbers regardless of the treatments available for it. Since patients with an MDR or XDR condition are limited in their treatment options, there is a huge need for new antibiotics against bacterial infections like TB.

The 3-ketosteroid-9 α -hydroxylase (KshAB) protein complex studied in this project hydroxylates the 9-position of steroid rings during the breakdown of steroids for energy in pathogenic bacteria (Figure 1a).⁶ It is comprised of two subunits referred to as

the hydroxylation reaction occurs. Each KshB subunit possesses an iron-sulfur cluster which is used to transfer the electrons from KshB to the iron-sulfur cluster in one subunit of KshA, which then transfers the electrons to the enzyme active site at the non-heme iron center of another subunit of KshA (Figure 1b).⁷ For efficient transfer of electrons between the iron-sulfur clusters, they must be 10-15 Å apart. This distance is expected for the entire protein complex when the KshA-KshB comes together, but the structure of the complex is not currently known.⁴ two configurations are believed to be the most likely of how the KshA and KshB dock and pass electrons from one subunit to the next subunit, however, the one that made the most sense with the docking program was utilized in this experiment (Figure 1b).

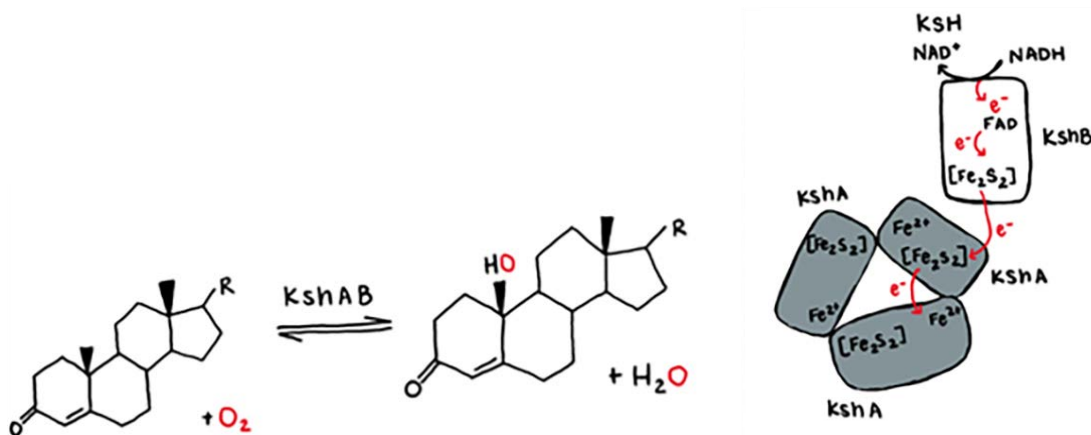


Figure 1: a) The hydroxylation of the KshAB protein complex. b) The proposed configuration of the protein complex demonstrates KshB converting NADH to NAD⁺ and using that electron to activate the KshA subunit.⁶

KshA – the oxygenase component that does the hydroxylation reaction – and KshB – the reductase component which transfers electrons to KshA. KshA is isolated as a trimer, where each monomer contains an iron-sulfur cluster and a non-heme iron center where

This project aims to identify and investigate potential binding sites between the KshA and KshB subunits of the protein complex KshAB. This work initially used computer programs such as ClusPro⁸⁻¹¹ for protein docking and Chimera and Pymol to visualize the protein

structure to identify possible locations where KshA and KshB interact. Subsequent work examined a mutation in the KshB subunit to investigate its impacts on the rate of electron transfer due to the mutation.

Methods

Protein Docking

The ClusPro Server was used to dock structures of KshA and KshB subunits. The KshA structure was obtained from the Protein Data Bank file 4QCK, while the KshB structure was determined based on a homology model from the Protein Data Bank file 2PIA from phthalate dioxygenase reductase constructed with the Phyre2¹³ server. Files of the KshA and KshB subunits were uploaded as the receptor and the ligand, respectively. The program allowed for modifications in docking parameters. After docking the proteins in ClusPro, distance measurements and investigation of possible amino acids to mutate were performed using the programs Pymol and Chimera programs. This protein docking process was repeated iteratively until a reasonable electron transfer distance was obtained (10-15 Å) and a particular amino acid was chosen to perform site-directed mutagenesis.

Site-Directed Mutagenesis

DNA primers for the KshB V246S mutation, shown below, were ordered from Invitrogen, and a Quik-Change II Site-Directed Mutagenesis kit was ordered from Agilent Technologies.

KshB_V246S Primer Sequence:

GCACAGCAGGTTTCATATTGAATCGTTTAAAGCCTGGAAAGCGA

KshB_V246S Reverse Compliment Primer Sequence:

TCGCTTTCAGGCTTTTAAACGATTCAATATGAACCTGCTGTGC

The protocol for site-directed mutagenesis was

adapted from the protocol included with the mutagenesis kit. The DNA primers created to reflect this change from V246S as well as the kit reagents were thawed out and diluted before the mutagenesis reaction and centrifuged down to ensure homogeneity. All the reagents were added into PCR tubes in the volumes indicated in (Table 1) for thermal cycling (Polymerase Chain Reaction) reaction. The thermal cycling (PCR) reaction ran in three segments to amplify this specific DNA segment being studied to a large enough amount for it to be studied in detail.

Segment 1: 95 °C for 30 sec (1 cycle)

Segment 2: 95 °C for 30 sec, 55 °C for 1 min, 68 °C for 6 min (18 cycles)

Segment 3: Hold at 4° C for infinity

10 µL of this undigested PCR reaction was saved from each sample to be run in a DNA gel before *DpnI* restriction enzyme was added to the remainder of each reaction to digest the methylated DNA to ensure that only the mutated DNA is left and incubated at 37 °C. XL-1 Blue Supercompetent cells, pUC18 control plasmid, and NZY+ broth were all thawed out and aliquoted appropriately during this hour. 1µL of the *DpnI* digest reaction was added to ¾ of the aliquoted cells while 1 µL of pUC18 control plasmid was added to ¼ of the aliquoted cells, flicked to combine the cells with the DNA, and incubated on ice. The cells were then heat shocked at 42 °C before being placed on ice to incubate again. NZY+ broth was added to each reaction and incubated with shaking to heat up the reaction before they were able to be plated.

Using the LB Amp plates, the pUC18 control reaction and pWhitescript reactions were appropriately aliquoted and the mutagenesis (V246S) reaction was appropriately aliquoted on LB Kan plates before being incubated overnight. The following morning

Reagent	1. pWhitescript Control	2. KshB_V246S	3. KshB_V246S
10X Reaction Buffer	5 μ L	5 μ L	5 μ L
DNA Template	2 μ L	2 μ L	2 μ L
Primer #1	1.25 μ L	1.25 μ L	1.25 μ L
Primer #2	1.25 μ L	1.25 μ L	1.25 μ L
dNTP Mix	1 μ L	1 μ L	1 μ L
Nuclease Free Water (PCR H ₂ O)	38.5 μ L	40.5 μ L	40.5 μ L
Pfu Ultra HF DNA Polymerase	1 μ L	1 μ L	1 μ L
Total Volume	50 μ L	52 μ L	52 μ L

Table 1: The amount of each reagent used to prepare the pWhitescript control and the KshB_V246S PCR products.

showed growth on both the control plates (pUC18 and pWhitescript) as well as the mutagenesis plates, which indicated a successful mutation from the valine residue to a serine residue.

A DNA gel was used to run the samples that contain DNA and stained them so they can be run through an imager and to provide confirmation of what the sample contained. A combination of agarose and 1X Tris-Acetate Ethylenediamine Tetraacetic Acid (TAE) buffer in a flask were swirled to combine before being placed in the microwave to fully dissolve. An SYBR-safe dye was also added to that flask and swirled to combine before the mixture was poured into a gel tray. Once the gel solidified, a good comb was placed to create wells for the samples to sit in. The gel was run

for 1 hour at 100 V and imaged on the molecular imager. The procedure for the mutagenesis of the KshB at position V246 created the basis of the in vitro lab work done in this study.

Protein Expression

Expression of KshA:

KshA plasmids were transformed into BL21-DE3 *E. coli* competent cells by adding 1 μ L of a plasmid to 50 μ L competent cells before being incubated on ice, heat shocked, and then incubated once again. SOC media was added into the cell-plasmid mixture and incubated with shaking to transform the KshA DNA into the BL21 cells. Lastly, the cells were plated onto LB-Kan plates and placed in an incubator overnight.

The following morning, there was growth on all the LB-Kan plates. Those colonies were used to prepare starter cultures by using a Bunsen burner and a sterile loop to scoop up isolated colonies from the plates and mix them into centrifuge tubes filled with LB media. This experiment produced five centrifuge tubes of inoculated media that were left to shake overnight in an incubator.

The inoculated starter cultures were taken out the next morning and mineral stock solution was added to each of the five pre-made flasks of LB media. A solution of kanamycin dissolved in PCR water was also added into the flasks before they were placed into incubators at 37 °C with shaking and checked in one-hour intervals to measure the absorbance (600 nm) using a PerkinElmer Lambda Bio+ Spectrophotometer (Table 3). The media was further inoculated using Isopropyl (beta)-D-1-thiogalactopyranoside (IPTG) after reaching an OD (absorbance) of 0.800 before being left in the incubator to shake overnight at 25 °C.

The five flasks of inoculated media were removed from the incubator the following morning. Once placed in centrifuge bottles and balanced, the media was spun down to receive a collective mass of 15.014 g of cells that were tan with rust-colored streaks as residue from the excess iron present in the mineral stock solution. The supernatant liquid was removed from the centrifuge bottles so the pellet could be scraped up with a spatula and transferred to a beaker to determine the collective weight of the pellets. Allocating one mL of resuspension buffer for one g of the pellet, approximately 20 mL of buffer was used in tandem with an autopipette to resuspend the cells in liquid for storage at -80°C.

Expression of KshB-V246S:

Starter cultures were produced by sterile

inoculation of LB-Kan media with colonies from KshB_V246S mutagenesis plates where the starter cultures were grown overnight at 37 °C. The next day, the starter colonies were centrifuged down to get pelleted cells, and the supernatant was dumped into a waste beaker. The pelleted cells were resuspended with a resuspension buffer containing RNase and then transferred into a microcentrifuge tube. A lysis solution was added to the microcentrifuge tube and inverted a few times to mix the solution before being incubated for five minutes. A neutralization solution was added to the microcentrifuge tube and inverted a few times to thoroughly combine the mixture until a solid white precipitate was left on the surface of the tube. Once combined, the mixture was centrifuged at 14000 rpm which transferred the precipitate to the sides of the microcentrifuge tube. The supernatant liquid was then transferred to a spin column and spun down in the centrifuge before a wash solution was added to the mixture twice and centrifuged down. The spin column was transferred into a microcentrifuge tube before an elution buffer was added to the column and allowed to incubate for two minutes. The eluted plasmid was collected into the microcentrifuge tube after being spun down for 2 minutes and subsequently stored in the freezer.

For immediate usage, the KshB-V246S plasmid was transformed into *E. coli* BL21-DE3 competent cells. Two samples of the KshB-V246S plasmid and two samples of BL21-DE3 cells were thawed on ice before the plasmid was added to each of the aliquots of cells. The plasmid-cell mixture was incubated on ice before getting heat shocked at 42°C and incubated on the ice again. The mixture was given SOC media while being incubated with shaking at 37°C before being plated on LB Kan plates.

The starter cultures were prepared after thawing out one sample of kanamycin and having LB media prepared from the day before and allowing it to reach room temperature overnight. The LB media was portioned into 10 mL stocks in centrifuge tubes (5 total) with an additional 10 μ L aliquot of kanamycin. With a sterile loop and Bunsen burner, the loop was sterilized in the flame and cooled until it reached room temperature to scoop up isolated colonies and mixed into the media. This process was repeated until all the centrifuge tubes had one colony in them or became inoculated. Both inoculated centrifuge tubes were incubated with shaking at 37°C overnight.

The inoculated starter cultures were removed from the incubator the following morning and mineral stock solution was added to each of the two flasks of LB media. Kanamycin was weighed out and dissolved in PCR water, so the solution could be added to each of the two flasks. The flasks were placed into 37 °C incubators with shaking for 30-minute – 1-hour intervals and the absorbance at 600 nm was measured (Table 8) using a PerkinElmer Lambda Bio+ Spectrophotometer. After the media reached an OD of 0.800, it was inoculated with IPTG and allowed to shake overnight at 30 °C.

For better long-term storage of the plasmid, the decision was to store the KshB_V246 plasmid in DH5 α cells. Two samples of the KshB_V246S plasmid and two samples of DH5 α cells were thawed on ice before the plasmid was added to each of the aliquots of cells. The plasmid-cell mixture was incubated on ice before getting heat shocked at 42°C and incubated on the ice again for another 5 minutes. The mixture was given SOC media while being incubated with shaking at 37°C and being plated on LB Kan plates in 100 μ L, 200 μ L, and 500 μ L volumes.

Since the DH5 α cells are better for long-term storage, the transformation of the mutated cells into the new cell type warranted a new plasmid as well. The starter colonies were centrifuged down to get pelleted cells and the supernatant was dumped into a waste beaker. The pelleted cells were resuspended with a resuspension buffer containing RNase and then transferred into a microcentrifuge tube. A lysis solution was added to the microcentrifuge tube and inverted a few times to mix the solution before being incubated. A neutralization solution was added to the microcentrifuge tube and inverted a few times to thoroughly combine the mixture until a solid white precipitate was left on the surface of the tube. Once combined, the mixture was centrifuged at 14000 rpm which transferred the precipitate to the sides of the microcentrifuge tube. The supernatant liquid was then transferred to a spin column and spun down in the centrifuge before a wash solution was added to the mixture twice and centrifuged down. The spin column was transferred into a microcentrifuge tube before an elution buffer was added to the column and allowed to incubate. The eluted plasmid was collected into the microcentrifuge tube after being spun down and subsequently stored in the freezer. The purified KshA and KshB served as pure samples of both subunits to ensure that any observed changes in the flow of the electrons could be attributed to the mutagenesis and not any impurities surrounding the protein.

Protein Purification

Purification of KshA:

1 mM phenylmethane sulfonyl fluoride (PMSF) and 0.3 mg/mL lysozyme were added to thawed KshA resuspended cells, and the mixture was incubated

on ice before being sonicated on ice for 6 cycles (30 seconds on/5 min off). The sonicated cells were then centrifuged at 18000 rpm for 30 minutes to separate the supernatant liquid from the cell debris that formed a pellet at the bottom of the bottle and the supernatant liquid was run through the Ni-NTA column with 20 mM potassium phosphate pH 8.0, using a step gradient of imidazole concentrations from 10 mM imidazole in the equilibration buffer, 25 mM imidazole in the wash buffer, and 250 mM imidazole in the elution buffer. Samples were concentrated with 10K centrifuge concentrators.

An SDS-PAGE was run on the Ni-NTA purified fractions. The samples were prepared by combining the KshA purification fractions (sample, wash, and elution) with SDS 2X buffer, centrifuged down before the samples were then heat shocked at 85 °C and added to the wells. Using a 1 mg/mL bovine serum albumin (BSA) stock solution, BSA dye reagent, and deionized water, the concentration of the KshA protein was determined through a Bradford Assay.

Purification of KshB-V246S:

The thawed cells were incubated with PMSF and lysozyme as with KshA and sonicated and centrifuged as with KshA. The cell extract was then loaded on a Ni-NTA column using Fast Protein Liquid Chromatography (FPLC) which was used to purify the KshA subunit with the same buffers as for KshA. The resulting KshB V246S mutation fractions were used in an SDS PAGE to ensure the isolation of the correct protein.

Enzyme Kinetics

The rate of NADH oxidation of the KshAB protein complex was measured by time-dependent UV-vis spectroscopy at 340 nm. The system contained the KshA

protein and a separately purified KshB-R286A protein with the following substrates, co-substrates, and buffer:

Reagents	Reference	Trial 1-3
0.16 μ M KshA	N/A	0.32 μ L
1.6 μ M R286D	N/A	1.6 μ L
100 μ M NADH	100 μ L	100 μ L
20 μ M Tris HCl	888.08 μ L	858.08 μ L
40 μ M Formestane	10 μ L	40 μ L

Table 2: *The composition of the reference solution and the solution containing both subunits.*

The initial slopes of the kinetic traces at 340 nm are used to determine the rate of enzymatic activity and electron transfer within the protein complex.

Results and Discussion

Protein Docking

The KshA and KshB subunits both contain an iron-sulfur cluster in which KshB takes an electron from NADH and passes it through the iron-sulfur cluster to reach KshA (Figure 1). When using Pymol, the specific distance that we were aiming to measure revolved around the distance between the iron-sulfur clusters in the subunits and ideally would be 10-15 Å in length to be the most probable distance for electrons to travel. The original docking model had a distance of 42.9 Å between the KshA and KshB subunits (Figure 2a). After several rounds of protein docking using ClusPro, there were two probable models with one presenting a distance of 14.4 Å (Figure 2b) and the

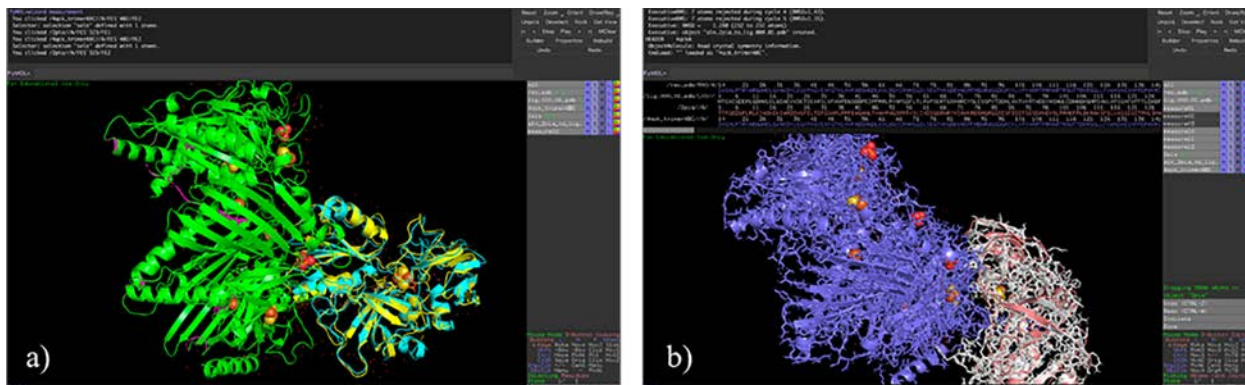


Figure 2: Comparison images of the (a) original docked KshAB complex interacting with one chain of the KshA subunit at 42.9 Å and (b) the more plausible KshAB complex at 14.4 Å.

other with a distance of 15.1 Å (Figure 3a). Ultimately, the model with a distance of 15.1 Å had more potential sites of interaction between the KshA and KshB, so all of the future mutations were done to this specific model.

There is one configuration of docking that seems most likely for the transfer of electrons from the KshB subunit to the KshA subunit (Figure 3b). There is a valine residue located at position 246 that was selected as a potential spot for mutation in this protein complex (Figure

3a). Valine 246 is a nonpolar residue located in the KshB subunit that is interacting with an arginine residue at position 106 in the KshA subunit, which is a positively charged amino acid. After several rounds of digital mutation, the valine residue could be mutated to a serine residue, which is polar, to observe any changes that may occur in the way that the bonding occurs in that position 246. Serine was selected because it was the only digital mutation that would have been of significant impact

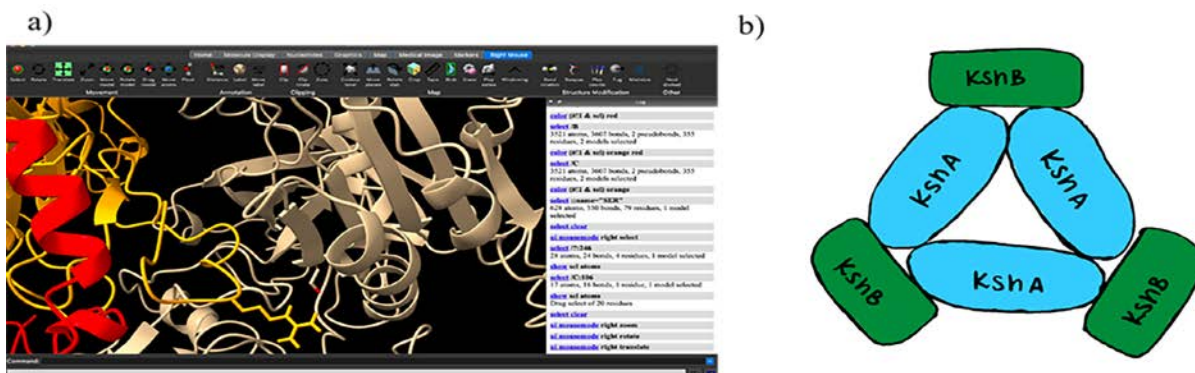


Figure 3: a) Screenshot of the Chimera interface. Chains A, B, and C of KshA have been highlighted in different colors. The yellow residue branching out of the KshA (Arg 106) is the nearest interaction to the tan residue branching out of the KshB (Ser 246). (b) The most likely possibility of the binding site in the KshAB protein complex.

without completely denaturing the surrounding proteins or being of the same nonpolar nature. This mutation would be changing the interaction from nonpolar to polar. The rest of this study focuses on how this mutation and the change in polarity will impact the protein complex’s ability to transfer electrons and provide more characterizing information about what this mutation would do.

Site-Directed Mutagenesis

Several rounds of mutagenesis were required to successfully incorporate the mutation to V246S, but ultimately successful mutagenesis was conducted. A DNA gel was run on the undigested PCR samples of the mutagenesis. The loading scheme was as follows:

1. Ladder (sample and 6X loading dye)
2. Empty
3. KshB_V246S PCR sample (sample and 6X loading dye)
4. KshB_V246S PCR sample (sample and 6X loading dye)
5. Empty
6. PCR Control sample (sample and 6X loading dye)

The site-directed mutagenesis was successful at changing the DNA sequence of KshB to introduce a serine at position 246 instead of a valine. Subsequent steps will determine if this mutation had the desired effect on protein function.

Protein Expression

Expression of KshA:

The KshA protein was expressed in *E. coli* BL21-DE3 competent cells. The time course of cell growth was observed in Table 3 with an optical density of cells being used as a metric for when to add the IPTG reagent to

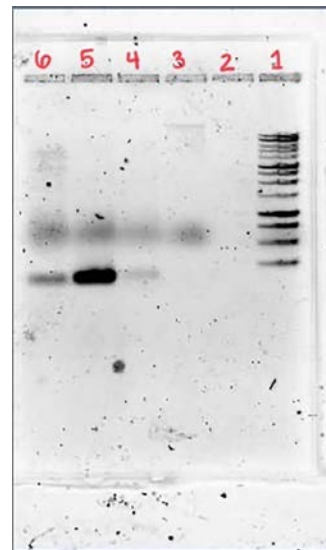


Figure 4: The DNA gel from the KshB_V246S mutagenesis shows that in comparison to the ladder, the KshB protein is present in the middle of the gel and that this mutation should be successful. of the KshB (Ser 246). (b) The most likely possibility of the binding site in the KshAB protein complex.

TIME	CONC.				
	Flask #1	Flask #2	Flask #3	Flask #4	Flask #5
11:08 AM	0.068	0.058	0.046	0.075	0.089
11:47 AM	0.114	0.161	0.103	0.112	0.086
12:59 PM	0.369	0.327	0.301	0.324	0.201
2:02 PM	1.865	1.030	1.026	0.993	0.608
2:13 PM	•	•	•	-	0.669
2:28 PM	•	•	•	-	0.742

Table 3: The progress for the absorbance at 600 nm of the inoculated media after several hours.

induce expression of the KshA protein.

Expression of KshB-V246S:

The KshB-V246S protein in *E. coli* BL21-DE3 competent cells. The time course of cell growth was observed in Table 4 with an optical density of cells being used as a metric for when to add the IPTG reagent to induce expression of the KshB-V246S protein.

Protein Purification

Purification of KshA:

Ni-NTA chromatography was used to purify KshA and an SDS-PAGE was run on the Ni-NTA purified fractions. The samples were added to the wells with the following loading scheme:

Well Number	Sample Type
2	Standard
4	Sample Fraction
7	Wash Fraction #1
9	Wash Fraction #2
11	Elution Fraction #1
13	Elution Fraction #2
15	Elution Fraction #3

The image below depicts the loading scheme starting with the standard on the left side and ending with the elution fraction #3. The green band indicates the region KshA is expected to appear in. The protein concentration of the KshA protein was determined through a Bradford assay using the following standard sequence shown in the table below (Table 5).

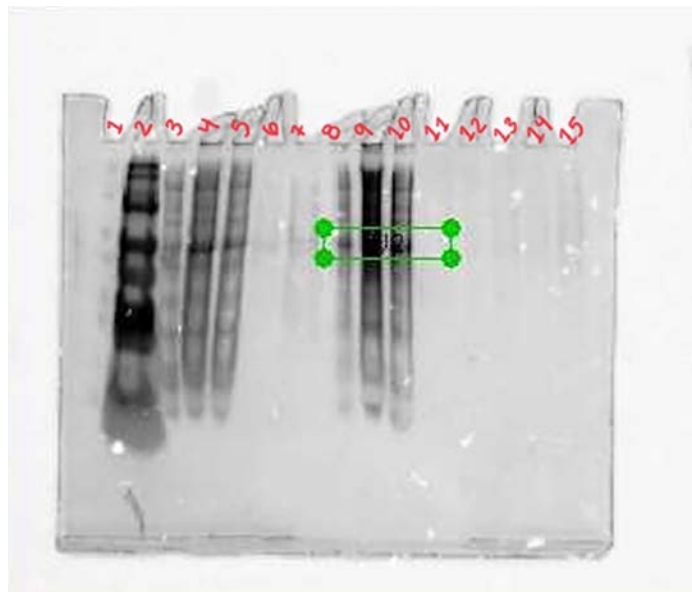


Figure 5: SDS-PAGE of purified KshA. The standard (lane 2) shows clear bands of the standard protein, while lanes 8-10 show a band (indicated by the green box) where the KshA is expected to show up.

TIME	CONC.	
	1 L Flask	500 µL Flask
10:21 AM	-	0.163
11:26 AM	0.074	0.228
12:39 PM	0.250	1.033
1:39 PM	1.203	-

Table 4: The progress for the absorbance at 600 nm of the inoculated media after several hours.

These steps all show that the *E. coli* bacteria could uptake and grow the wild-type and mutated plasmids expressing the protein of interest.

Deionized (DI) Water	800 μ L	798 μ L	796 μ L	794 μ L	792 μ L	790 μ L
BSA Stock	0 μ L	2 μ L	4 μ L	6 μ L	8 μ L	10 μ L
BSA Reagent	200 μ L					
Total Volume	1000 μ L					
Absorbance	0.000	0.072	0.363	0.372	0.408	0.685

Table 5: The amount of each reagent used to prepare the standard curve used to calculate the concentration of the KshA protein.

The standard curve of the BSA standard stock solution produced the following graph (Figure 6) which was then used to calculate the concentration of the KshA of 0.110 mg/mL.

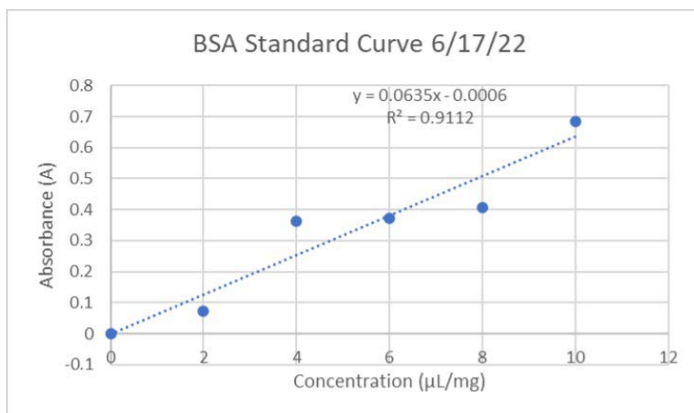


Figure 6: The graph plotting the absorbance versus concentration for the standard protein concentration as well as the R^2 value and resulting equation

Expression of KshB-V246S:

The KshB-V246S protein was isolated via Ni-NTA chromatography, and an SDS-PAGE was done to confirm the relative size and purity of the protein complex. The

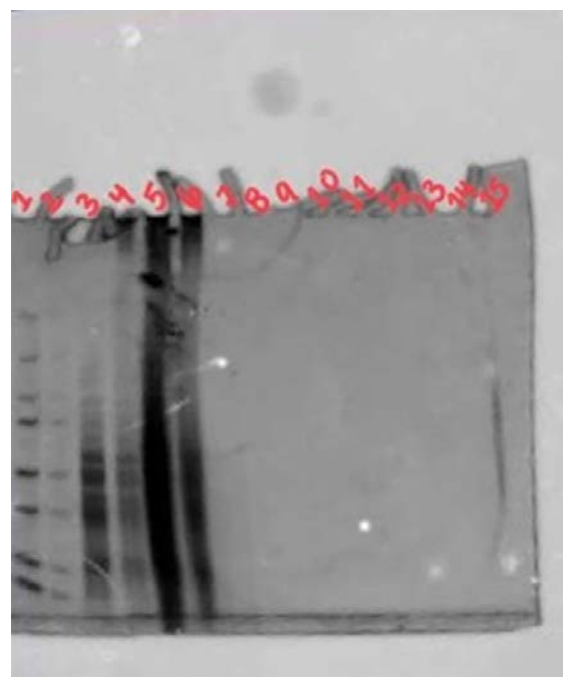


Figure 7: The SDS-PAGE of purified KshB V246S. The standard (lane 1, left side) shows clear bands of the standard protein, while lanes 3-7 show bands of where the KshB is expected to be.

protein purification separated the proteins of interest from the cell extract and then SDS-PAGE and Bradford's assays were used to measure the purity and quantity of

each protein produced.

Enzyme Kinetics

Initial analysis of enzyme kinetics was conducted using a previously mutated sample of KshB with a mutation at position 286 where arginine was made into an aspartic acid (R286D). As shown in Figure 1, NADH becomes NAD⁺ once the KshB subunit takes the electron from the compound and uses the electron to transfer to the KshA subunit through both of their iron-sulfur clusters. The KshA subunit then transfers that electron to the enzyme's active site.

By varying the concentration of the substrate (Table 2), the degradation of NADH becomes easily observable and that information can give more context to the function of the protein. The raw data (Figure 8) shows the degradation of the NADH plotted by the decreasing absorbance on the y-axis and the time span of 15 minutes (600 seconds) on the x-axis.

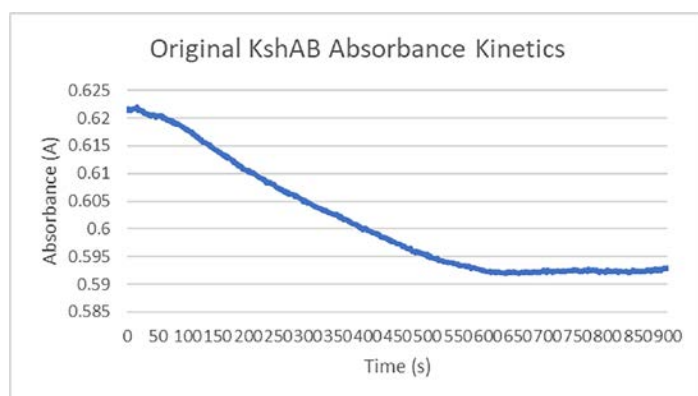


Figure 8: The degradation of NADH (absorbance) over the span of 600 seconds.

The modified graph of degradation of NADH in the protein complex (Figure 9) shows how quickly the NADH degraded within the first 300 seconds to provide

an R² value of 0.9946, which can be used to assess the correlation between the speed of the absorbance over time at different concentrations.

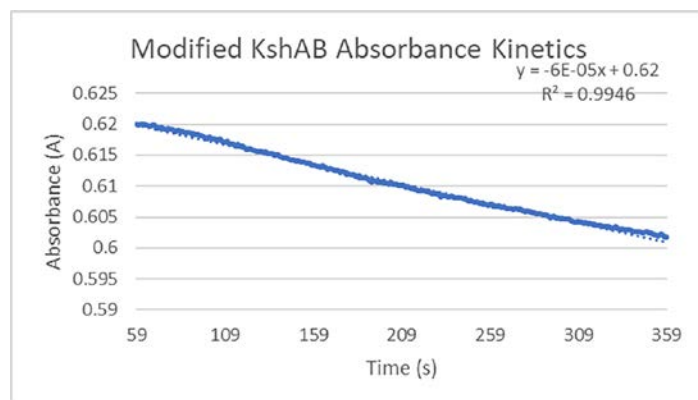


Figure 9: The plot of absorbance of the NADH present in the complex over the first 350 seconds of the experiment.

These kinetic assays allow us to determine the rate of the hydroxylation reaction in the enzyme complex. Future work will be able to study the KshA-KshB_V246S mutant complex in more detail to determine how the electron transfer is altered in the complex. This information will help guide additional studies on the location of the KshA-KshB binding site.

Conclusions and Outlook

This project has allowed for the development of the V246S mutation in the KshB subunit that is being tested in combination with KshA and NADH to inhibit the flow of electrons within the protein complex. This development, if successful, will be the backbone for developing a single treatment for tuberculosis to replace the current standard of taking multiple treatments, which can be costly in terms of the medication's price and how much time is needed to take these medications. In terms

of multi-drug resistant and extensively drug-resistant cases of tuberculosis, this would be a novel drug in hopes of reducing the amount of maintenance required to continuously treat the disease.

With the remaining amount of time in the semester, I expect to be able to continue this research project through a Bradford assay on the resulting fractions to be able to figure out the concentration of the V246S-KshB protein. Once I've purified and concentrated the protein, I can then begin observing the enzyme kinetics by varying the concentration of the steroid substrate and analyzing them by plotting the data to perform a Michaelis-Menten kinetic analysis and determine K_M , V_{max} , and k_{cat} for this system and conditions. If successful, this research could be used to develop one singular treatment for tuberculosis that would replace the need for multiple drugs, reducing the out-of-pocket cost of infected individuals and their family members and reducing the amount of time spent taking those medications every day.

References

1. *Center for Disease Control Treatment for TB Disease* <https://www.cdc.gov/tb/topic/treatment/tbdisease.htm> (accessed 2021-08-3)
2. *World Health Organization Tuberculosis Fact Sheet* <https://www.who.int/news-room/fact-sheets/detail/tuberculosis> (accessed 2021-08-03)
3. Miao, V.; Davies, J. Actinobacteria: The Good, the Bad, and the Ugly. *Antonie van Leeuwenhoek* 2010, 98 (2), 143–150. <https://doi.org/10.1007/s10482-010-9440-6>.
4. Petrusma, M.; van der Geize, R.; Dijkhuizen, L. 3-Ketosteroid 9 α -Hydroxylase Enzymes: Rieske Non-Heme Monooxygenases Essential for Bacterial Steroid Degradation. *Antonie van Leeuwenhoek* 2014, 106, 157–172. <https://doi.org/10.1007/s10482-014-0188-2>.
5. Hu, Y., Geize, R., et al. (2010). 3-Ketosteroid 9-hydroxylase is an essential factor in the pathogenesis of *Mycobacterium tuberculosis*. *Molecular Microbiology*, 75 (1), 107-121.
6. Szaleniec, M., Wojtkiewicz, A., et al. (2018). Bacterial steroid hydroxylases: enzyme classes, their functions, and comparison of their catalytic mechanisms. *Applied Microbiology and Biotechnology*, 102 (19), 8153-8171.
7. Desta, I. T.; Porter, K. A.; Xia, B.; Kozakov, D.; Vajda, S. Performance and Its Limits in Rigid Body Protein-Protein Docking. *Structure* 2020, 28 (9), 1071-1081.e3. <https://doi.org/10.1016/j.str.2020.06.006>.
8. Kozakov, D.; Hall, D. R.; Xia, B.; Porter, K. A.; Padhorny, D.; Yueh, C.; Beglov, D.; Vajda, S. The ClusPro Web Server for Protein-Protein Docking. *Nat Protoc* 2017, 12 (2), 255–278. <https://doi.org/10.1038/nprot.2016.169>.
9. Vajda, S.; Yueh, C.; Beglov, D.; Bohnuud, T.; Mottarella, S. E.; Xia, B.; Hall, D. R.; Kozakov, D. New Additions to the ClusPro Server Motivated by CAPRI. *Proteins* 2017, 85 (3), 435–444. <https://doi.org/10.1002/prot.25219>.

10. Kozakov, D.; Beglov, D.; Bohnuud, T.; Mottarella, S. E.; Xia, B.; Hall, D. R.; Vajda, S. How Good Is Automated Protein Docking?: Automated Protein Docking. *Proteins* 2013, 81 (12), 2159–2166. <https://doi.org/10.1002/prot.24403>.
11. Kelley, L. A.; Mezulis, S.; Yates, C. M.; Wass, M. N.; Sternberg, M. J., The Phyre2 web portal for protein modeling, prediction and analysis. *Nat. Protoc.* 2015, 10 (6), 845-58.
12. Capyk, J. K.; D'Angelo, I.; Strynadka, N. C.; Eltis, L. D. Characterization of 3-Ketosteroid 9 α -Hydroxylase, a Rieske Oxygenase in the Cholesterol Degradation Pathway of Mycobacterium Tuberculosis. *Journal of Biological Chemistry* 2009, 284 (15), 9937–9946. <https://doi.org/10.1074/jbc.M900719200>.
13. Hu, Y.; van der Geize, R.; Besra, G. S.; Gurcha, S. S.; Liu, A.; Rohde, M.; Singh, M.; Coates, A. 3-Ketosteroid 9 α -Hydroxylase Is an Essential Factor in the Pathogenesis of Mycobacterium Tuberculosis. *Molecular Microbiology* 2010, 75 (1), 107–121. <https://doi.org/10.1111/j.1365-2958.2009.06957.x>.



MALIKA CRUICKSHANK

Chemistry, Professional Chemistry Concentration

Malika Cruickshank graduated in 2023 with a degree in Chemistry, concentration in Professional Chemistry, and two minors, in Mathematics and Psychology. Her research took place over the course of three years under the mentorship of Dr. Sarah R. Soltau (Chemical Sciences) and with the support of multiple grants, including the Adrian Tinsley Program summer research grant and the SEISMIC grant through the National Science Foundation. Malika presented variations of this research at the 2022 National Conference on Undergraduate Research (NCUR) and at BSU's Adrian Tinsley Program (ATP) Symposium. She plans to pursue an MD/DO to practice pediatric surgery.